A study of the dusk convection cell's response to an IMF southward turning

Tadahiko Ogawa, Nozomu Nishitani, Natsuo Sato, Hisao Yamagishi, Mike Pinnock, Jean-Paul Villain, George Sofko, Oleg Troshichev

A study of the dusk convection cell's response to an IMF southward turning

Nozomu Nishitani,[1] Tadahiko Ogawa,[1] Natsuo Sato,[2] Hisao Yamagishi,[2]
Mike Pinnock,[3] Jean-Paul Villain,[4] George Sofko,[5] and Oleg Troshichev[6]

Received 26 February 2001; revised 27 June 2001; accepted 27 June 2001; published 29 March 2002.

[1] One example of the response of ionospheric convection and the polar cap boundary to a sudden change in the interplanetary magnetic field (IMF) orientation has been studied by using ground magnetometers, the Super Dual Auroral Radar Network (SuperDARN), and Defense Meteorological Satellite Program (DMSP) particle detectors when the IMF suddenly changed from northward (+6 nT) to strongly southward (−19 nT) at 1716 UT on 5 September 1995. The B_z component was fairly constant for ~2 hours before and ~25 min after the sudden IMF change. The convection flow changed almost simultaneously over a global extent. This initial change of the convection pattern can be characterized by a sudden formation of a large flow vortex in the afternoon sector. This agrees with the earlier findings by *Ruohoniemi and Greenwald* [1998] and *Ridley et al.* [1998]. On the other hand, the response of the polar cap boundary (or its proxy) is more complicated. The Saskatoon radar, located in the late morning sector, observed an equatorward shift of the cusp scatter region simultaneously with the initial response of the convection flows. The DMSP particle data also showed a simultaneous equatorward expansion of the auroral oval in the 2100 magnetic local time (MLT) sector. The radar and particle data indicate the immediate equatorward expansion of the precipitation regions in the noon and premidnight sectors. About 10–20 min after the initial change, there were changes observed in the dusk region, namely, an equatorward expansion of the current reversal boundary observed by the Greenland magnetometer chain in the dusk sector between 1740 and 1750 UT and an equatorward expansion of the convection reversal boundary detected by the Stokkseyri, Halley, and Syowa radars. The delayed responses were observed 18-8 min before a substorm onset was recorded at midlatitude stations at 1756 UT. These observations indicate that there were two kinds of ionospheric responses to the southward turning of the IMF; the first response is the formation of the convection vortex and the equatorward shift of the polar cap boundary at noon and at ~2100 MLT, and the second response is the equatorward expansion of the convection reversal boundary in the dusk sector. We make the case that the first response is associated with the propagation of magnetosonic waves and that the second response is consistent with the *Cowley and Lockwood* [1992] picture of the redistribution of the newly created open flux in the polar cap region. *INDEX TERMS:* 2463 Ionosphere: Plasma convection; 2784 Magnetospheric Physics: Solar wind/magnetosphere interactions; 2431 Ionosphere: Ionosphere/magnetosphere interactions; 2437 Ionosphere: Ionospheric dynamics; *KEYWORDS:* Ionospheric convection, IMF southward turning, polar cap boundary

1. Introduction

[2] Ionospheric convection at high latitudes is largely controlled by the orientation of the interplanetary magnetic field (IMF) as a result of the solar wind–magnetosphere–ionosphere interaction. There have been a number of statistical studies of ionospheric convection pattern as a function of IMF, using data from satellites [e.g., *Weimer*, 1995], incoherent scatter radars [e.g., *Senior et al.*, 1990], and HF radars [*Ruohoniemi and Greenwald*, 1996].

[3] Although it is important to study the statistical pattern of the ionosphere under steady IMF conditions as an equilibrium state, the solar wind is highly variable, and the Earth's magnetosphere is continuously affected by the time-varying solar wind. In this case the dynamics of the ionospheric convection associated with sudden changes in the IMF provide a key to the magnetospheric reconfiguration process.

[4] There have been a number of studies of the ionospheric convection response associated with southward turnings of the IMF. *Etemadi et al.* [1988] correlated the IMF observed by the satellites and dayside ionospheric flows measured by an incoherent scatter radar. They found a clear relationship that depends strongly on the latitude and local time. *Todd et al.* [1988] used the same data set as *Etemadi et al.* [1988] and investigated the timescale of the response of the high-latitude dayside ionospheric

[1]Solar-Terrestrial Environment Laboratory, Nagoya University, Toyokawa, Japan.
[2]National Institute of Polar Research, Tokyo, Japan.
[3]British Antarctic Survey, Cambridge, England, UK.
[4]Laboratoire de Physique et Chimie de l'Environnement, CNRS, Orléans, France.
[5]Department of Physics and Engineering Physics, University of Saskatchewan, Saskatoon, Saskatchewan, Canada.
[6]Arctic and Antarctic Research Institute, St. Petersburg, Russia.

0148-0227/02/2001JA900095

flow to changes in IMF B_z. *Saunders et al.* [1992] studied magnetic field changes on the ground associated with IMF variations and estimated the response time to the solar wind changes as a function of magnetic local time. The above studies showed that the speed of longitudinal propagation of convection pattern changes is within the range of 1–5 km/s.

[5] On the other hand, *Ruohoniemi and Greenwald* [1998] reported an event when the IMF B_z abruptly changed from positive to negative. They concluded that the disturbance of convection propagates very rapidly from the dayside to the nightside within a time span of 2 min and that the reconfiguration of the convection pattern also occurs very rapidly, in ~2–4 min. *Ridley et al.* [1998], using the AMIE algorithm and ground magnetic data, also reported that after an IMF southward turning, the two-cell convection pattern forms very quickly and does not change its shape after its initial formation. Their results appear to be different from the previous results by, for example, *Etemadi et al.* [1988]. *Lockwood and Cowley* [1999] commented that *Ridley et al.*'s [1998] result clearly shows the expansion of the convection cell, which is consistent with the earlier results by, for example, *Lockwood et al.* [1986], *Etemadi et al.* [1988], and *Todd et al.* [1988]. *Ridley et al.* [1999] replied that the expansion of the convection cell is an incorrect interpretation of the data. *Khan and Cowley* [1999] showed from the statistical analysis of the European Incoherent Scatter (EISCAT) data that the averaged travel speed of the disturbance (6.8 km/s) is faster than the previous results, but there is still a finite delay of 10 min from the dayside to the nightside. These arguments have not led to definitive conclusions.

[6] *Lockwood and Cowley* [1999], referring to their Figure 3, discussed the difference between their model and that of *Ridley et al.* [1998] in terms of the response of the polar cap boundary to the IMF change. In their discussion the behavior of the polar cap boundary plays a significant role. *Lopez et al.* [1999] showed in their three-dimensional MHD simulation that the convection pattern across the entire polar cap begins to change a few minutes after the arrival of the southward IMF, whereas the onset of the equatorward motion of the open-closed field line boundary depends on the local time, with equatorward motion of the midnight boundary delayed by ~20 min relative to the onset of the boundary motion at noon. However, there have been no observations that confirm this simulation result.

[7] There have been several studies to discuss the ionospheric responses to the IMF changes using different approaches. *Hairston and Heelis* [1995] used Defense Meteorological Satellite Program (DMSP) driftmeter data to discuss the response time of the IMF changes. Owing to the limitation of the satellite passes, the response time had an uncertainty of 10–30 min. *Sandholt et al.* [1994] and *Ohtani et al.* [1997] discussed the response of the auroral activity to the IMF changes by using the ground-based and satellite auroral image data, respectively, although their observations were limited to the dayside region.

[8] One reason why this kind of observational analysis is difficult is that the IMF variation cannot be controlled. *Khan and Cowley* [1999] tried to evaluate the response time of the ionospheric convection as a function of local time. However, they encountered some difficulty in determining the time lag because their results revealed a more complex response to the IMF in the postdusk region, with V_E (eastward component of the plasma velocity) switching from negative to positive as B_z became more negative. As in other physical systems, the response of the magnetosphere-ionosphere system to IMF B_z changes is clarified when those changes occur in a stepwise, rather than gradual, manner.

[9] In this paper we present one example where the IMF B_z changes sign from positive to negative very abruptly, while other parameters do not change much and B_z remains fairly constant for ~30 min before and after the event. We show data from several ground magnetometers and Super Dual Auroral Radar Network (SuperDARN) HF radars and describe the characteristics of the response associated with the B_z change. In fact, we show that the ionospheric response associated with the IMF B_z change has a two-stage structure. In the discussion we provide interpretation of the

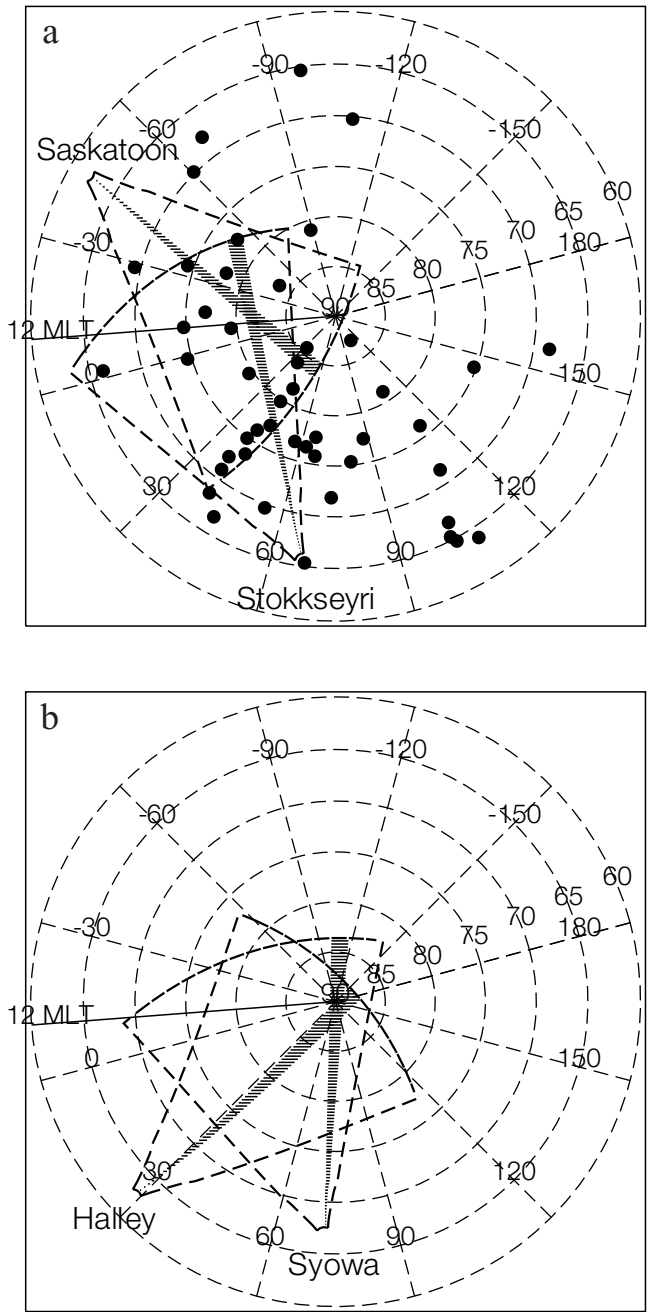

Figure 1. Distribution of SuperDARN radars in the (a) Northern and (b) Southern Hemispheres and the ground magnetometers in the Northern Hemisphere. The magnetic latitude and longitude are given in the altitude adjusted corrected geomagnetic coordinate (AACGM) system, which is an updated version of the Polar Anglo-American Conjugate Experiment (PACE) geomagnetic coordinate system [*Baker and Wing*, 1989]. Also shown are the fields of view of beam 6 of the Saskatoon, beam 12 of the Stokkseyri, beam 8 of the Halley, and beam 13 of the Syowa radars.

Table 1. Magnetic Stations Used in This Study

Station Code	Geographic Latitude	Geographic Longitude	Geomagnetic Latitude	Geomagnetic Longitude	Source
ALE	82.50	297.65	87.12	107.22	Intermagnet
CBB	69.12	254.97	77.52	−53.01	Intermagnet
MBC	76.32	240.64	80.99	−88.92	Intermagnet
RES	74.69	265.10	83.57	−43.68	Intermagnet
BLC	64.32	263.99	74.37	−33.86	Intermagnet
FCC	58.76	265.91	69.41	−28.67	Intermagnet
PBQ	55.28	282.26	66.30	−1.76	Intermagnet
THL	77.47	290.77	85.70	32.72	Intermagnet
GDH	69.25	306.47	76.14	40.48	Intermagnet
NAQ	61.16	314.56	66.70	43.75	Intermagnet
BRW	71.32	203.38	70.27	−109.94	Intermagnet
CMO	64.86	212.16	65.38	−96.91	Intermagnet
ABK	68.36	18.82	65.33	102.52	Intermagnet
SOD	67.37	26.63	63.92	107.91	Intermagnet
YKC	62.48	245.52	69.84	−60.49	WDC-A
FSP	61.75	238.77	67.80	−68.30	WDC-A
LRV	64.18	338.30	65.35	67.83	WDC-A
BJN	74.50	19.20	71.45	109.23	WDC-A
NAL	78.92	11.93	76.15	112.61	WDC-A
TRO	69.66	18.95	66.65	103.70	WDC-A
KIR	67.83	20.42	64.70	103.35	WDC-A
HIS	80.62	58.05	75.24	144.77	AARI
DIK	73.55	80.58	68.47	156.20	AARI
AMK	65.60	322.37	69.65	54.71	Greenland
ATU	67.93	306.43	74.91	39.04	Greenland
DMH	76.77	341.37	77.40	87.74	Greenland
DNB	74.30	339.78	75.34	81.00	Greenland
FHB	62.00	310.32	68.40	39.48	Greenland
GHB	64.17	308.27	70.95	38.36	Greenland
KUV	74.57	302.82	81.54	44.64	Greenland
NRD	81.60	343.30	81.04	107.04	Greenland
SCO	70.48	338.03	71.87	73.62	Greenland
SKT	65.42	307.10	72.39	37.79	Greenland
STF	67.02	309.28	73.52	41.76	Greenland
SVS	76.02	294.90	83.96	35.63	Greenland
UMQ	70.68	307.87	77.23	44.09	Greenland
UPN	72.78	303.85	79.81	42.11	Greenland
MCE	72.58	326.10	75.83	66.59	MAGIC
MCG	72.57	321.55	76.58	62.32	MAGIC
MCN	73.93	322.38	77.70	65.77	MAGIC
MCW	72.00	317.25	76.80	56.99	MAGIC
CD	64.20	283.40	74.58	1.12	MACCS
CH	64.10	276.80	74.75	−10.79	MACCS
CY	70.50	291.40	79.58	18.48	MACCS
GH	68.60	264.10	78.22	−36.50	MACCS
IG	69.30	278.20	79.44	−8.40	MACCS
RB	66.50	273.80	76.92	−16.76	MACCS

data and consider the physical mechanisms required to cause the observed responses.

2. Instrumentation

2.1. Solar Wind Parameters

[10] The location of the IMP 8 satellite in the geocentric solar magnetospheric (GSM) coordinate system was [29.8, −14.3, −3.1] (R_E) at 1630 UT and [30.0, −13.8, −1.2] (R_E) at 1830 UT on 9 September 1995. IMP 8 was obviously in the interplanetary medium during the period of interest. There were also the Wind ([100.25, 4.47,−15.67] at 1630 UT and [100.05, 6.29, −15.23] at 1830 UT) and Geotail ([21.08, −17.47, 4.63] at 1630 UT and [−21.48, −16.59, 2.68] at 1830 UT) satellites in the interplanetary medium. These satellite data will be used to supplement the IMP 8 data.

2.2. Ionospheric and Ground-Based Data

[11] Figure 1 indicates the distribution of the high-latitude ground magnetic stations and the fields of view of the four SuperDARN radars, two (Saskatoon and Stokkseyri) in the Northern Hemisphere and two (Halley and Syowa) in the Southern Hemisphere, used in this study. The magnetic latitude and longitude are given in the altitude adjusted corrected geomagnetic coordinate (AACGM) system, which is an updated version of the Polar Anglo-American Conjugate Experiment (PACE) geomagnetic coordinate system [*Baker and Wing*, 1989]. Table 1 lists the many magnetic stations used in this study. We use magnetic data with 1-min time resolution, although some stations have higher time resolution (e.g., 5 s for MACCS stations and 20 s for Greenland stations). The radars were operated in the SuperDARN Common Program mode, where each radar was scanned through 16 viewing directions every 2 min, from west (beam 0) to east (beam15) for the Saskatoon, Halley, and Syowa radars and from east (beam 15) to west (beam 0) for the Stokkseyri radar. Other radars (Kapuskasing, Goose Bay, and Finland) were also operating during this period but unfortunately did not produce sufficient echoes. Therefore we will not use the data from these radars.

[12] In addition to the ground magnetograms and SuperDARN radar data, DMSP particle data are used to discuss the precipitation

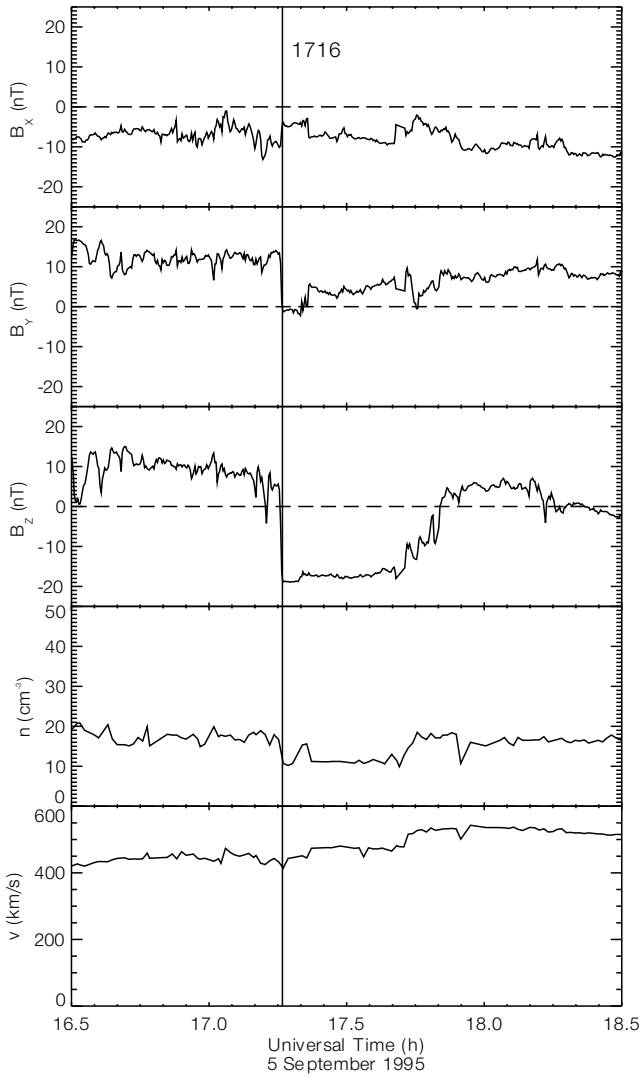

Figure 2. Variations of interplanetary magnetic field and solar wind density and speed observed at the IMP 8 satellite from 1630 to 1830 UT on 5 September 1995. The data are given in the geocentric solar magnetospheric (GSM) coordinate system.

characteristics of the high-latitude ionosphere during the sudden IMF southward turning.

3. Observations

3.1. Solar Wind Parameters

[13] Figure 2 shows the variation of the IMF components and the solar wind density and velocity at IMP 8. The most notable change is the sudden southward turning of the B_z component at 1716 UT. Before this time, B_z was positive (centered between 5 and 10 nT) for 2 hours, then changed from +6 nT to −19 nT within 30 s. Although there are changes in the other components at the same time, these changes are relatively small compared with the B_z change: B_x changed from −10 nT to −4 nT, and B_y changed from 13 nT to −1 nT. (Later, we show that the effect of this B_y change is smaller than the B_z effect.) The solar wind density decreased from 17 to 11 cm^{-3} simultaneously with the B_z change. It increased again to 15 cm^{-3} at 1720 UT and then decreased to 11 cm^{-3} at 1722 UT. The solar wind velocity increased gradually during the period of interest.

[14] There was a precursor B_z negative change at 1713 UT and also a slight decrease in B_z at 1708 UT. The Wind satellite, located ~100 R_E upstream from the Earth, observed similar changes. On the other hand, the Geotail satellite, located closer to the Earth but farther away from the Sun-Earth line, did not observe the corresponding precursor changes, although for the rest of the period Geotail showed characteristics similar to IMP 8 and Wind. One explanation for this discrepancy is that the portion of the solar wind carrying these precursor changes impinged on only a part of the Earth's magnetopause; the effect would then be spatially localized.

[15] After 1716 UT the B_z component stayed constant (centered at about −19 nT) for ~25 minutes, then began to increase gradually at 1741 UT. This profile provides a condition suitable for monitoring the response of the ionosphere to the IMF change.

3.2. Ground Magnetometers, SuperDARN, and DMSP Observations

[16] Figure 3 shows stacked magnetograms from the selected stations, one in the cusp region (IG), one in the polar cap near the geomagnetic pole (THL), two in the nightside region (HIS and DIK), and others in the dusk sector (GHB and AMK). It can be seen from the cusp region Ym component magnetogram (IG) that the initial response began at 1726 UT, indicating that it is most probable that the time delay from the IMP 8 satellite to the ground is ~10 min.

[17] Figure 4 shows the range-time-profile (RTP) plots of the line-of-sight velocities obtained by four SuperDARN radars, two in the Northern Hemisphere and two in the Southern Hemisphere. The radar fields of view cover the range from the late morning sector (Saskatoon) through the afternoon sector (Halley) to the evening sector (Stokkseyri and Syowa).

[18] Both the ground magnetograms and SuperDARN radar data show rather complicated changes. In the following we will describe the event in two ways; one is in terms of the convection flows, and the other is in terms of the polar cap (or convection reversal) boundaries.

3.2.1. Characteristics of convection flows. [19] As already mentioned, the cusp region magnetogram (IG) showed the initial response at1726 UT. The polar cap (THL) and the nightside (HIS) magnetograms also show initial responses at 1726 UT, demonstrating that the disturbance propagated across the polar cap immediately. This characteristic agrees with the results by *Ridley et al.* [1998] and *Ruohoniemi and Greenwald* [1998]. The Xm (north-south) components on the dusk magnetograms indicate initial responses almost simultaneously (with a delay of <2 min) with the noon and midnight magnetograms and development of the east-west equivalent current system. The Ym (east-west) components show irregular signatures. This is largely because the formation of the Dp-2 current system mainly affects the Xm component in the dusk sector, with only minor factors affecting the Ym component. Detailed discussion of the duskside characteristics will be given in the next section.

[20] Figure 5 shows the equivalent current vector distribution in the northern high-latitude region at 1728, 1730, 1735, 1740, 1750, and 1755 UT, obtained from the ground magnetograms. The baselines are set to be the values at 1726 UT. In fact, the initial changes had already begun at 1726 UT. However, the initial deviation at 1726 UT is relatively small compared to the later changes and the fluctuation level before 1726 UT, so that the selection of background values before 1726 UT does not change the characteristics of Figure 5. The horizontal component magnetic field vectors have been rotated clockwise by 90° to produce equivalent current vectors.

[21] By 1728 UT the gradual formation of the Dp-2 current system had already started. Although the development of the current system at this stage looks localized to the dayside region in Figure 5, the initial response started on a global scale at 1726

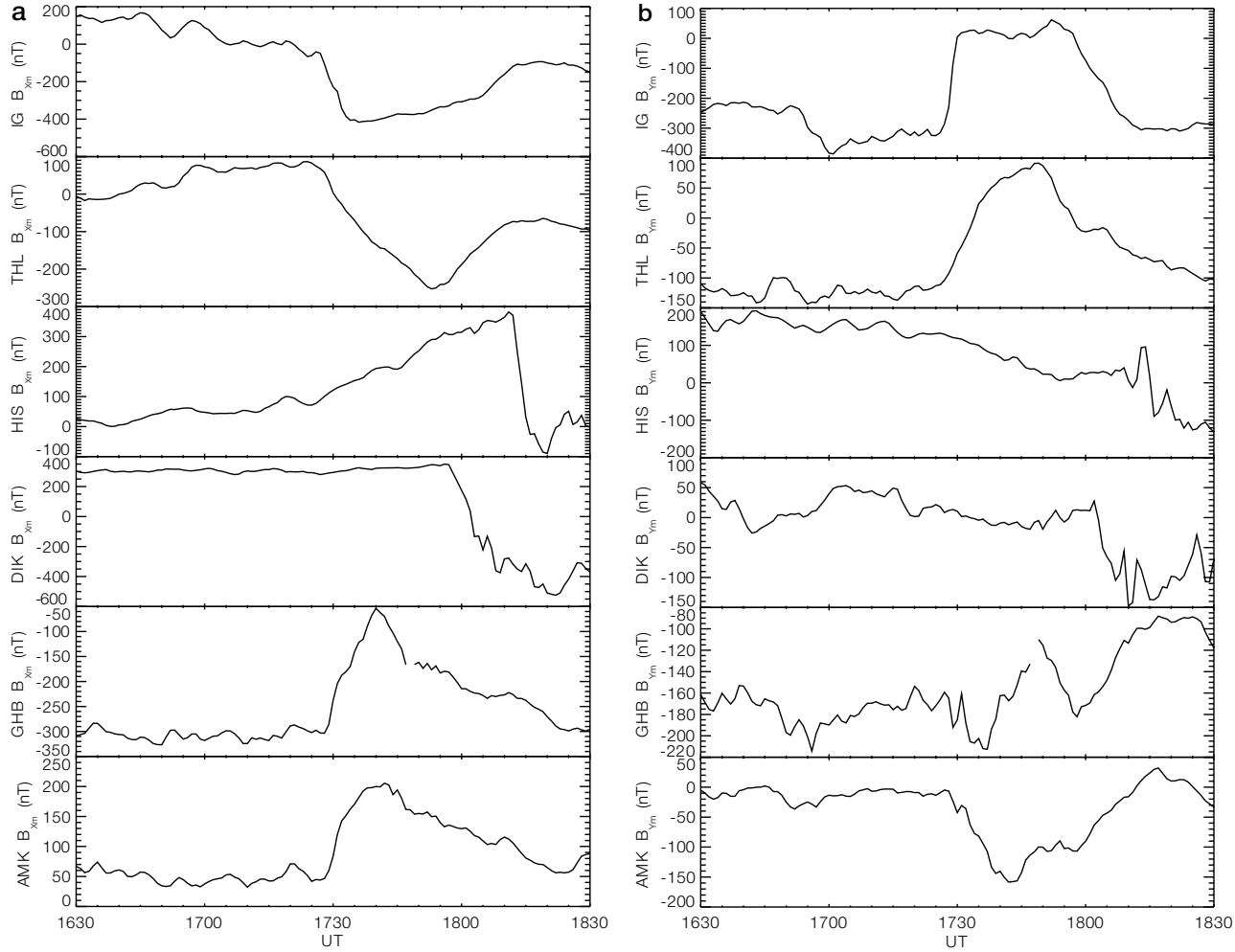

Figure 3. (a) Xm and (b) Ym component magnetograms from the selected stations, one in the cusp region (IG), one in the polar cap near the geomagnetic pole (THL), two in the nightside region (HIS and DIK), and others in the dusk sector (GHB and AMK) from 1630 to 1830 UT on 5 September 1995.

UT, as confirmed in Figure 3. The development of the intensity of the current system with time is seen in Figure 5. Details of the equivalent currents in the dusk region will be discussed in the next section.

[22] Within the SuperDARN network the initial response was observed by the Saskatoon radar at 1728:51 UT, at ~1100 magnetic local time (MLT). (This is not shown in Figure 4 because the first response was observed in beam 7 data, whereas the panel shows beam 6 data. Beam 7 did not show enough echoes throughout the whole period of interest, so it is not suitable for showing the overall profile.) This response time agrees well with the ground magnetometer data in the dayside region, considering the 2-min sampling rate of the radar. The transition period of the change (1728–1730 UT) also corresponds to that of the largest change in the IG magnetogram.

[23] Corresponding convection changes were observed by other radars almost simultaneously. The Stokkseyri radar (~1700 MLT) saw no measurable delay in the propagation of the enhanced electric field. The 1728 UT Saskatoon scan reveals poleward flow in beam 7 at 1728:51 UT; Stokkseyri saw enhanced flows toward the radar in beam 8 (not shown in Figure 4) almost simultaneously at 1728:50 UT. The Halley radar (~1500 MLT) saw line-of-sight velocity enhancement in the eastern part of the field of view at 1729:42UT (beam 14). We cannot say if the flows were enhanced at 1728:56UT (beam 8), because the flows were expected to be orthogonal to that beam. The Halley radar recorded the line-of-sight velocity pattern, which can be interpreted in terms of the uniform eastward flow in the higher latitude and westward flow in the lower latitude; this also agrees with the flow pattern in the dusk sector of the Northern Hemisphere. With this observation we expect that during the 1728- to 1730-UT scan the flows are in the east-west direction, that is, orthogonal to beam 8, by assuming that the flow pattern did not change much in a few minutes. The Syowa radar (~1800 MLT) showed a change in the line-of-sight velocity pattern between the 1726 and 1728 UT scans, but the pattern was disordered, so that it is difficult to say the earliest time that the flow change was observed.

[24] The velocity variations detected by the Halley and Syowa radars slightly following the initial change are rather complicated. Figure 6 shows line plots of the Halley and Syowa line-of-sight velocities of various range gates of beams 8 and 12 (Halley) and 3 and 13 (Syowa). Both radars show responses coincident with the responses in the Northern Hemisphere. Halley shows westward (returning) flows accelerating at 1730 UT (beam 12, 1050- to 1250-km ranges, corresponding to 69.5°–71.5° latitude). In addition to the westward flow related to the formation of the afternoon convection cell, there was also

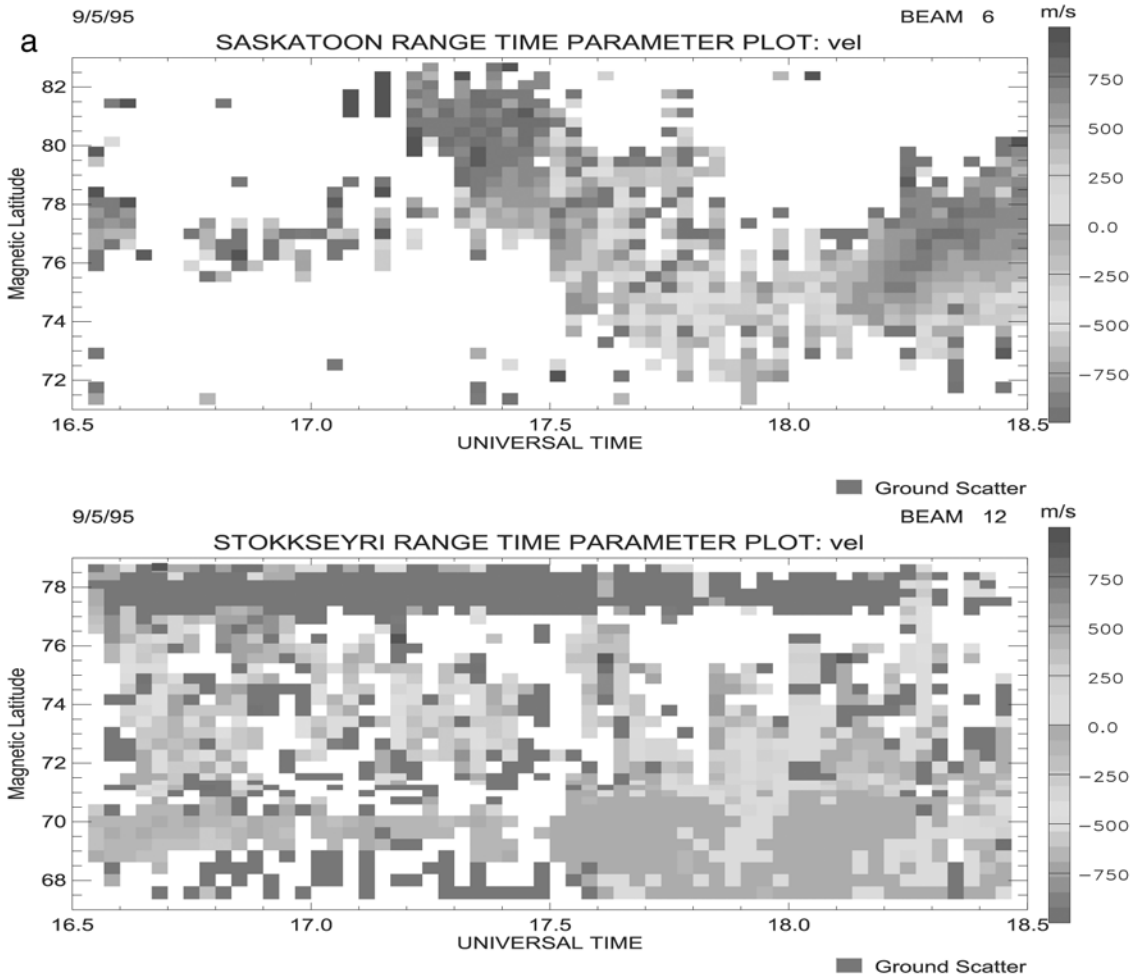

Figure 4. Range-time profile (RTP) plots of the line-of-sight velocities observed at beam 6 of the Saskatoon, beam 12 of the Stokkseyri, beam 8 of the Halley, and beam 13 of the Syoma radars from 1630 to 1830 UT. The positive velocities are toward the radar, and negative velocities are away from the radar. The gray area indicates a ground scatter region. See color version of this figure at back of this issue.

a transient impulse at 1732 UT (e.g., beam 8, 1150- to 1400-km ranges, corresponding to 70.5°–72.5° latitude). Note that a transient event at 1732 UT is also seen by SKT magnetogram: it may be the signature, proposed by *Araki* [1994], of transients at the magnetopause, caused by either pressure changes or reconnection events. There is also a Syowa response at 1734 UT (beam 13, 600- to 850-km range, corresponding to 71°–72° latitude) that decays away; this might also be the signature proposed by *Araki* [1994].

3.2.2. Characteristics of polar cap and convection reversal boundary motion. [25] In addition to the sudden change in the flow direction, the Saskatoon radar observed an equatorward shift of the scatter region, probably corresponding to the cusp scatter region if the cusp can be regarded as a hard target [e.g., *Milan et al.*, 1998; *Baker et al.*, 1995]. This agrees with the result of *Sandholt et al.* [1994] reporting a strong relationship between IMF B_z variations and latitudinal movements of the dayside aurora. The equatorward boundary of the cusp scatter can be confirmed from the particle data obtained by the DMSP satellites. Figures 7 and 8 show F12 and F10 DMSP spectrograms during 1729–1749 UT and 1737–1757 UT, respectively. Both satellites crossed the polar region of the Northern Hemisphere from the nightside (~2100 MLT) to the dayside (0900–1000 MLT), with a relative time delay of 8 min. We can confirm that the equatorward boundary of the DMSP ion dispersion region (denoted by vertical lines in Figures 7 and 8) coincides with the equatorward boundary of the scatter region observed by the Saskatoon radar in the same MLT sector (not shown) within 1° of latitude.

[26] Another important point that can be deduced from Figures 7 and 8 is that the nightside auroral oval expanded equatorward between the passes of the two satellites. The poleward boundary of the auroral oval, denoted in Figures 7 and 8, shifted equatorward from 67.5° latitude to 65.4° latitude (~2°) in ~7 min. It should be noted that there is an MLT difference between two DMSP passes, 2036 and 2118 MLT. Calculation based on the statistical Feldstein auroral oval [*Holzworth and Meng*, 1975] shows that the maximum MLT effect in the present case is 0.5° in latitude, indicating that there is obviously an enhanced equatorward shift of the auroral oval in the nightside region. If we assume that the MLT effect for the two DMSP passes is 0.5°, then the net equatorward expansion speed of the auroral oval boundary is 0.42 km/s (1.6° in 7 min). This value is comparable to the equatorward expansion speed of the Saskatoon scatter region boundary, which is ~0.3 km/s (3° in 18 min).

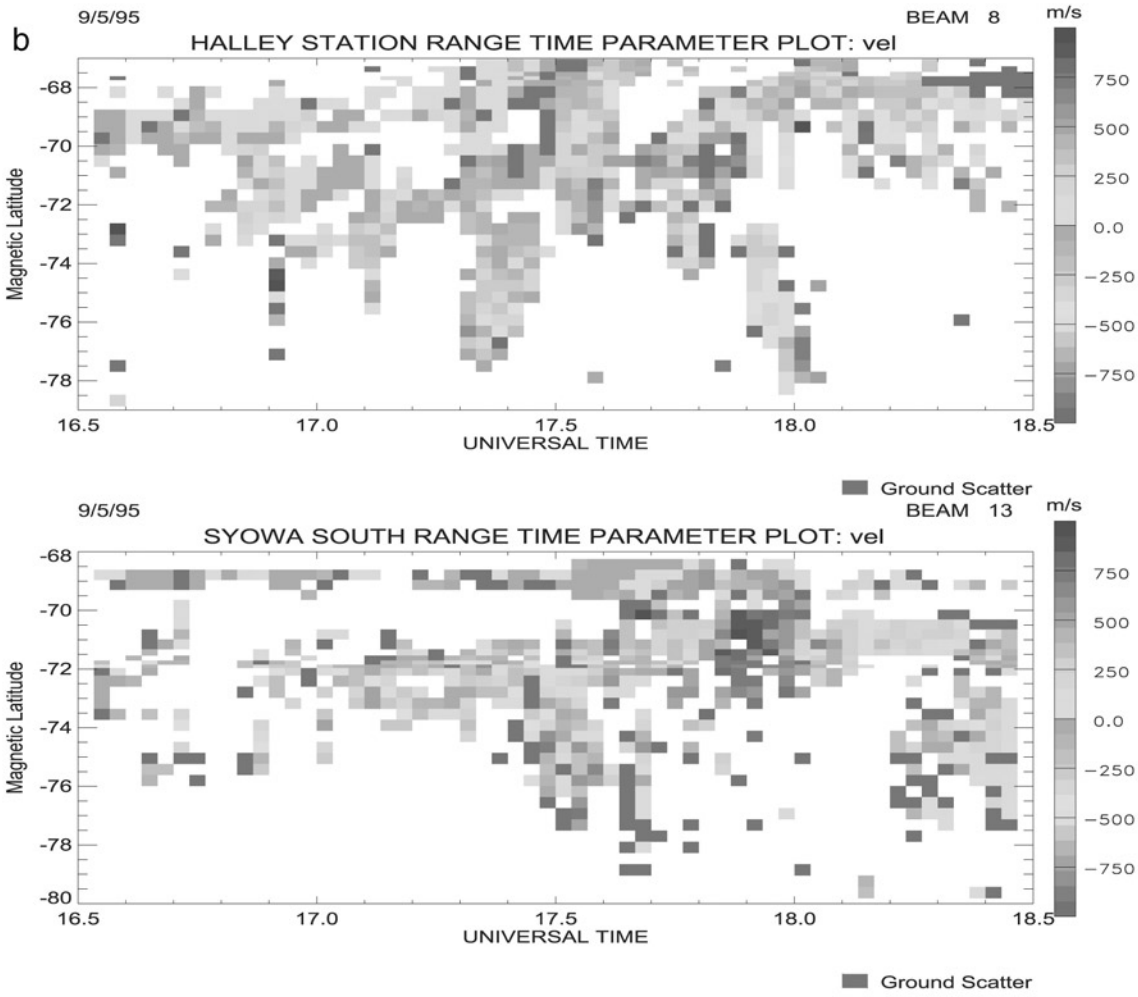

Figure 4. (continued)

[27] Poleward of the auroral oval, F12 and F10 each show a soft electron zone (SEZ) [*Lyons et al.*, 1996], the equatorward boundary of which can be identified by a discontinuous decrease in $\gtrsim$1 keV plasma sheet electrons almost to the detector background level. *Lyons et al.* [1996] stated that large portions of the SEZ seem to be on open field lines, although they are not completely certain about this conclusion. In any case, we obviously observed the sudden equatorward shift of the whole auroral oval. This means that the nightside polar cap boundary responds to the IMF change very quickly. Unfortunately, we have no radar data in the nightside region, so detailed analysis of the motion of the nightside polar cap boundary is impossible.

[28] Although the response of the polar cap boundaries in the noon and premidnight sectors is almost immediate, the response in the dusk sector is more complex. The equivalent current system in Figure 5 shows that between 1740 and 1750 UT, which is $\sim$10–20 min after the first change, the distribution of the equivalent current system began showing the expansion of the convection cells. The expansion seems to be both in longitude and in latitude. We cannot reliably comment on the longitudinal shift; the east-west component of the magnetic field is most sensitive to the longitudinal shift of the current vortex, but it is often contaminated by the fringing effect of the field-aligned currents [e.g., *Kamide et al.*, 1976].

[29] In latitude, there is an equatorward expansion of the convection cells, or, in other words, equatorward shift of the current reversal boundary dividing eastward and westward electrojets. Figure 9 shows this in greater detail, giving a high-resolution (1-min) stack plot of Greenland West chain equivalent current vectors, located at 1530 MLT. It can be seen that the boundary between the eastward and westward electrojets shifts equatorward by 2.5° between 1735 and 1750 UT. This equatorward expansion of the convection reversal boundary was also seen in the Stokkseyri RTP plot in Figure 4. The boundary dividing the eastward (toward, light blue) and westward (away, green) flow regions shifted to lower latitudes between 1740 and 1750 UT.

[30] Figure 10 shows the DMSP F13 spectrograms for the 1745- to 1755-UT pass. This path crossed approximately along the dawn-dusk meridian,close to the Stokkseyri beam 12 coverage area. From the F13 data it can be seen that the separatrix, given by the equatorward boundary of the SEZ region defined by a discontinuous decrease in $\gtrsim$1-keV plasma sheet electrons (denoted by a vertical line), matches the convection reversal boundary deduced from Stokkseyri data within 1° of latitude.

[31] Figure 11 shows the stacked plot of the variations of Saskatoon cusp scatter boundary, Greenland West chain convection reversal boundary, and Stokkseyri radar convection

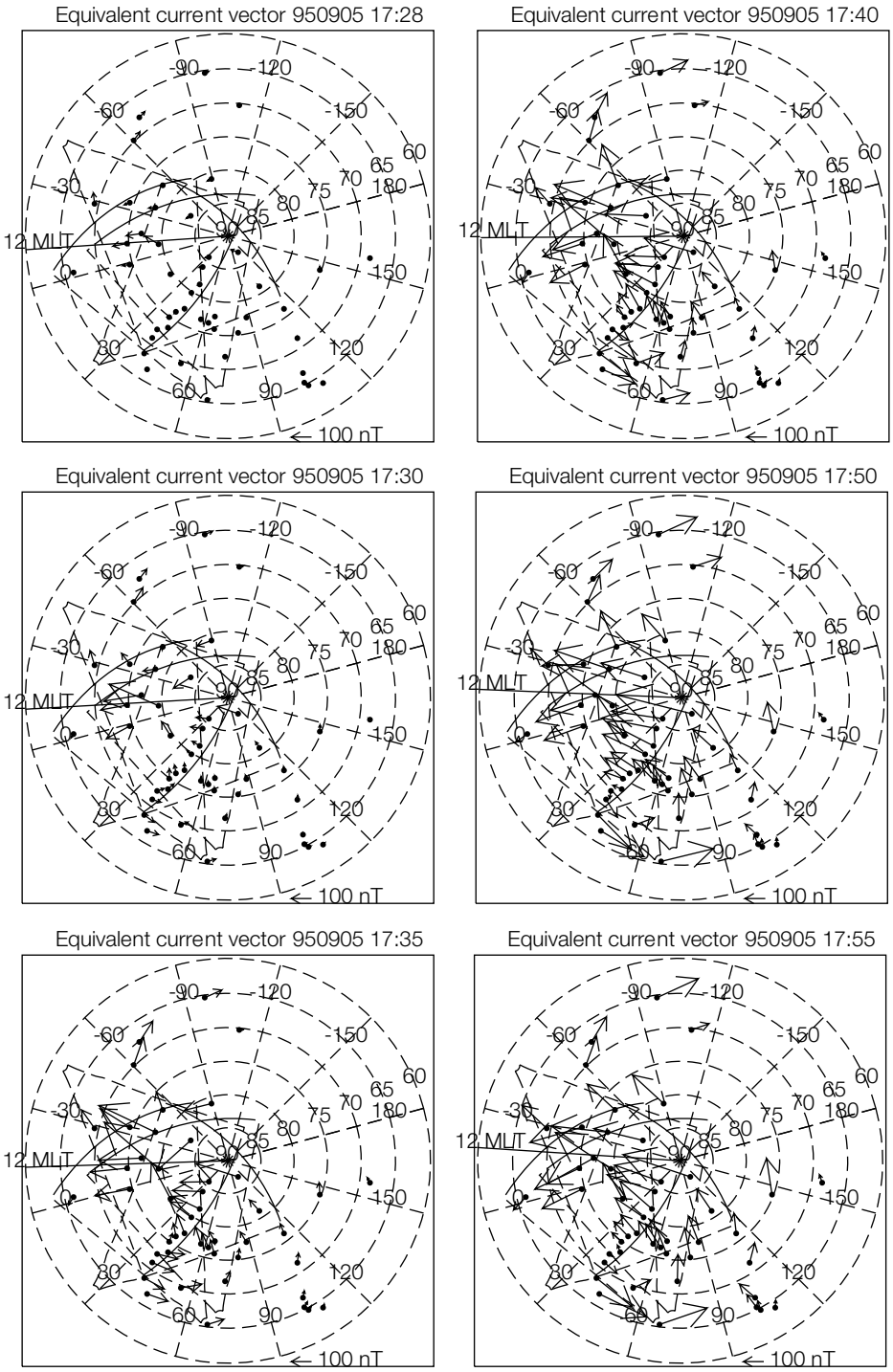

Figure 5. Equivalent current distribution in the northern high-latitude region at 1728, 1730, 1735, 1740, 1750, and 1755 UT, obtained from the ground magnetograms. The baselines are set to the values at 1726 UT. The horizontal component magnetic field vectors are rotated clockwise by 90° to produce equivalent current vectors.

reversal boundary at 60° longitude (~1700 MLT). Note that only the data after 1730 UT were shown. The convection reversal boundaries could not be defined before 1730 UT since the flow pattern was completely different during northward IMF. Saskatoon scatter boundary has the data before 1730 UT, but we have plotted the equatorward boundary of scatter showing cusp characteristics for B_z southward cusp only in order to avoid confusing two different regimes. Under southward IMF it marks the equatorward boundary of the cusp particle precipitation [*Baker et al.*, 1995]. However, during the B_z northward period (prior to 1730 UT) under lobe cell reconnection the particles and reconnection electric field arrive in the ionosphere and then trigger equatorward flow (with some azimuthal component depending on IMF B_y). So the equatorward boundary of the

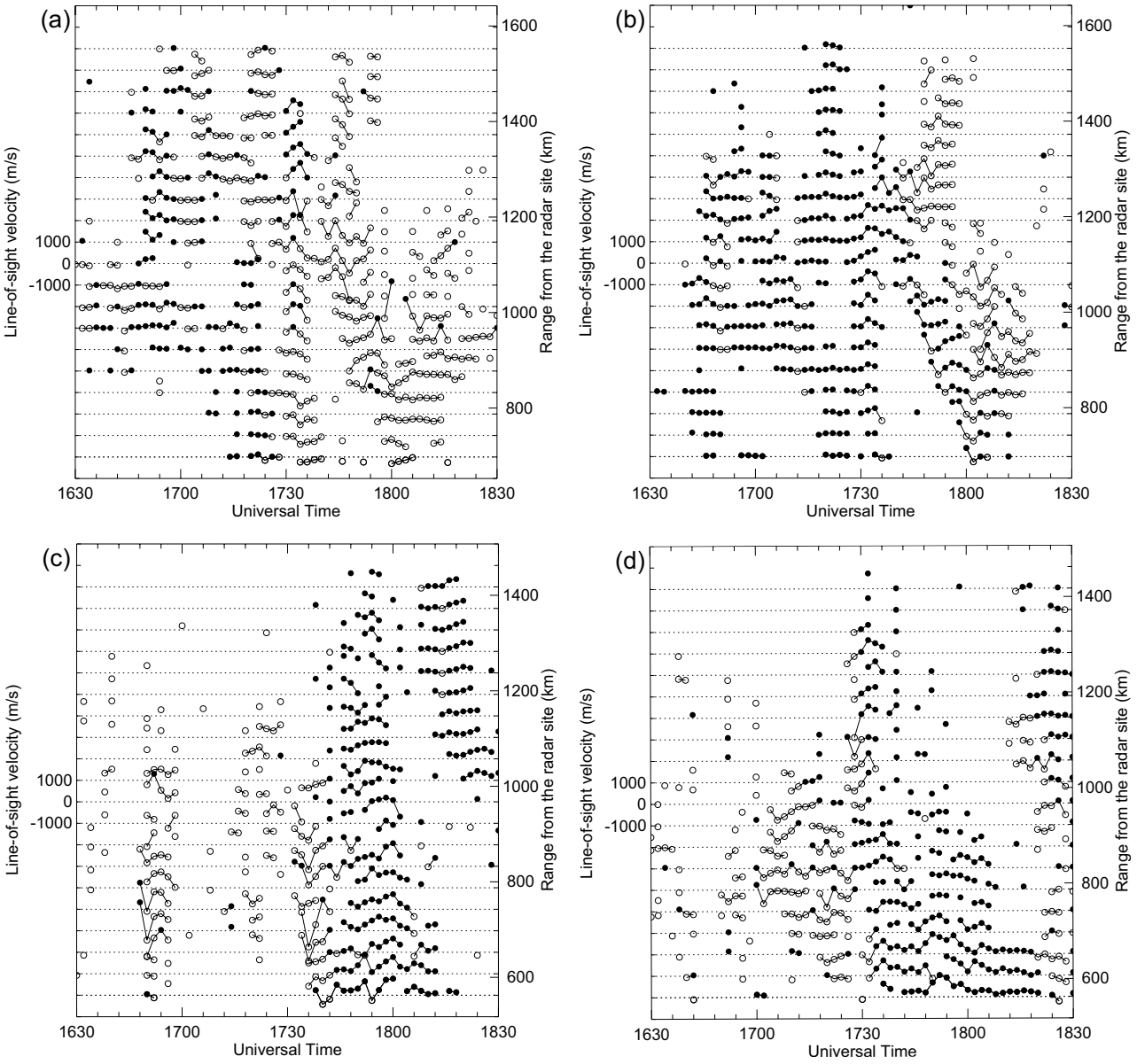

Figure 6. Line plots of Halley and Syowa line-of-sight velocities of beams (a) 8 and (b) 12 (Halley) and (c) 3 and (d) 13 (Syowa). The positive (toward the radar) velocities are denoted by solid circles, and the negative (away from the radar) velocities are denoted by open circles.

scatter is some distance equatorward of where the highest energy cusp ions are arriving in the ionosphere. In any case, we expect that the dayside polar cap boundary prior to 1730 UT stayed constant under steady northward IMF, as we can see in the top panel of Figure 4. Two vertical bars with ticks show DMSP auroral oval regions at ~2100 MLT in the Northern Hemisphere; the higher boundaries are supposed to correspond to the separatrix. The diamond shows the DMSP F13 separatrix in the dusk sector, as identified by the SEZ equatorward boundary.

[32] Both the dayside cusp scatter region and the nightside DMSP separatrix show fast (<10 min) responses to the IMF, whereas the Greenland West chain and Stokkseyri convection reversal boundaries show slower (>10 min) responses. Obviously, there is a time delay between the equatorward shift of the polar cap boundaries at noon and at ~2100 MLT and that of the convection boundary at ~1700 MLT. The characteristics of the responses following a sudden southward turning of the IMF are summarized in Table 2.

[33] The variations corresponding to the polar cap motion are also seen in the Southern Hemisphere. The Halley beam 12 in Figure 6 shows the equatorward motion of the boundary between positive (toward component) and negative (away component) flows from the 1300-to 1000-km range (71.5°–69.0° latitude), starting at 1742 UT, which matches the Stokkseyri equatorward movement of the convection reversal boundary. The Syowa beam 3 (Figure 6) may show the equatorward expansion of the boundary although there are more fluctuations.

[34] We should also mention that the delayed response in the convection boundary at ~1700 MLT is not related to a major substorm expansion onset. Both the high-latitude magnetograms in the Northern Hemisphere and the midlatitude magnetograms in the

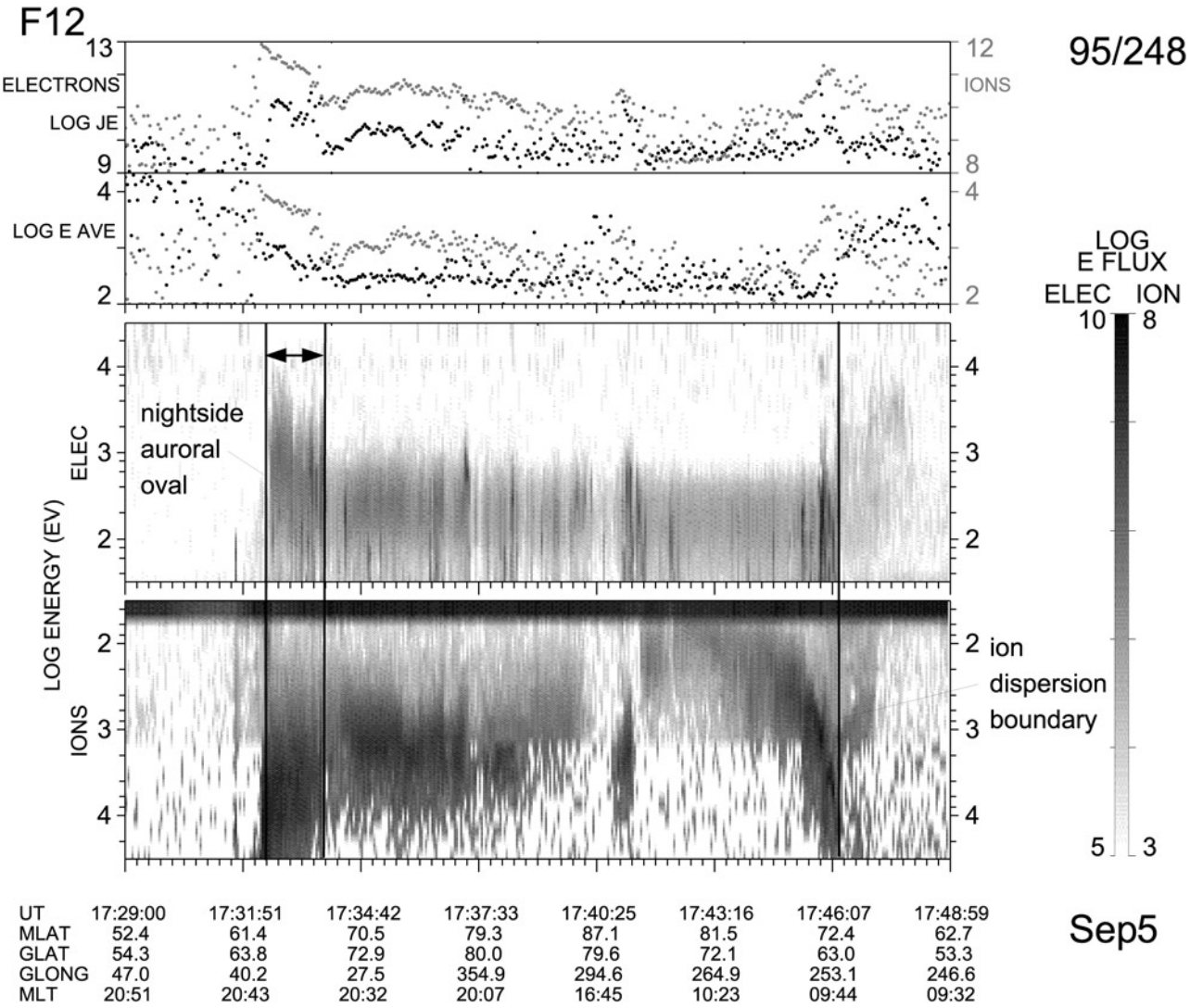

Figure 7. DMSP-F12 ion and electron spectrograms during 1729–1749 UT. The vertical line on the right side shows the equatorward boundary of the cusp precipitation region. The nightside auroral precipitation region is indicated by the arrow.

Southern Hemisphere, located in the nightside sector, indicate that the earliest expansion onset was 1756 UT.

4. Discussion

4.1. Overview and Interpretation of the Whole Event

[35] Sometime after the B_z southward change encounters the magnetopause, an eastward electric field is imposed on the dayside cusp region, accelerating plasma into the polar cap. The cusp region magnetometers and the Saskatoon radar show this electric field through the measurement of large poleward flows in the noon and prenoon sector.

[36] This electric field is sensed across the polar cap, at least as far as HIS (3300 km from IG), almost instantaneously. We have no clear way of knowing to what lower latitude the nightside response extends, but note that nightside (midnight) auroral latitude magnetograms (e.g., DIK) do not show any response at this time. However, this could be because there is insufficient ionospheric conductivity. (All other magnetograms examined are from the solar illuminated ionosphere.) Note that there is no measurable delay in the propagation of the enhanced electric field between the Saskatoon/Stokkseyri radars. In the present case we mean "no measurable delay" with respect to one radar scan period (2 min). Overall, the convection changes seen by the radars agree in time with the equivalent current changes seen on the magnetograms.

[37] This nearly simultaneous sensing of the cusp electric field throughout the polar cap and afternoon auroral oval is strongly suggestive of the magnetosonic wave/incompressible ionosphere mechanism. The equivalent current pattern shows that the afternoon convection cell formed immediately (1726 UT) and then intensified (enhanced flow speeds) over the next 25 min. This agrees with the findings of *Ridley et al.* [1998].

[38] The gradient of change in any of the magnetic field components is maximum in the cusp region (e.g., IG) and decreases toward dusk. We do not know the reason for this. Some candidates are the effects of conductivity gradients or field-aligned currents. This is a subject of future studies.

[39] Next, we focus on the afternoon convection cell response and, in particular, the behavior of the polar cap boundary motion,

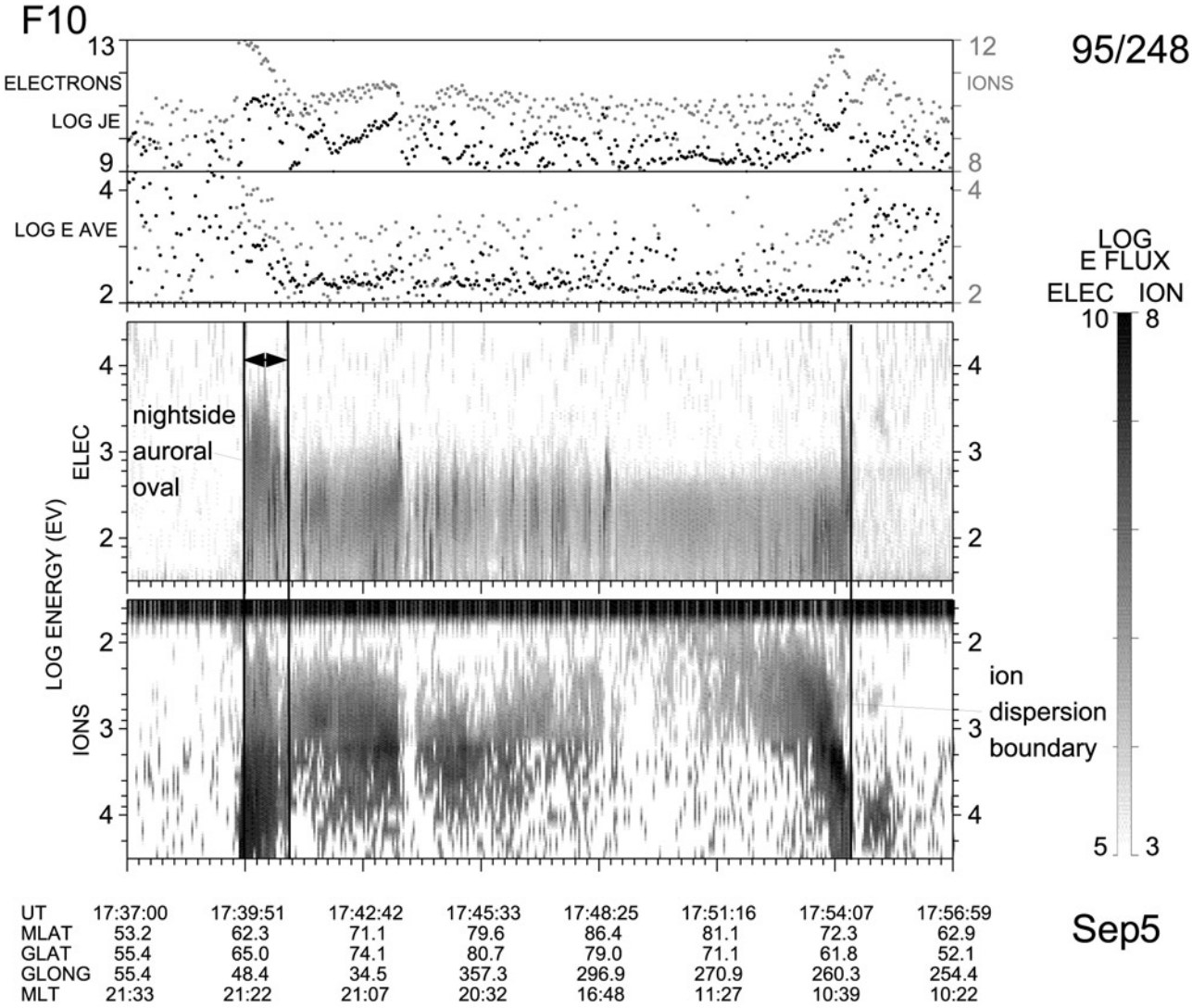

Figure 8. DMSP F10 ion and electron spectrograms during 1737–1757 UT. The vertical line on the right side shows the equatorward boundary of the cusp precipitation region. The nightside auroral precipitation region is indicated by the arrow.

which plays an important role in the framework of the *Cowley and Lockwood* [1992] paper (hereinafter referred to as CL1992). The gross movement of the polar cap boundary is shown by (1) Saskatoon cusp scatter moving equatorward (supported by evidence from DMSP); (2) Greenland West chain equatorward motion of the convection reversal boundary at 40°E longitude (~1530 MLT) (Figure 9); (3) Stokkseyri convection reversal boundary equatorward motion at ~60°E longitude (~1700 MLT) (supported by the evidence from DMSP); and (4) DMSP F10 and F12 equatorward motion of high-latitude auroral oval boundary (~2100 MLT).

[40] The data show that the polar cap boundary moves equatorward first at 1730 UT at the ~1100-MLT (Saskatoon radar data) and the ~2100-MLT meridians (DMSP F10 and F12 data), then the convection reversal boundary shifts equatorward at the Greenland West chain (1735 UT) and at the Stokkseyri radar (1742 UT). If we take the movement of the convection reversal boundary as a proxy for the polar cap boundary, the measurements lead to an estimated phase velocity of the 3.8 km/s for the significant polar cap boundary motion.

[41] The net equatorward motion of the convection reversal boundaries at the Greenland West chain and Stokkseyri radar occurred between 1740 and 1750 UT. This is obviously delayed as compared to the polar cap boundary motion at Saskatoon radar, where the largest boundary motion happened between 1730 and 1745 UT.

[42] There may appear to be a contradiction between seeing the onset of the enhanced reconnection electric fields everywhere and yet the evolution of the polar cap boundary taking many minutes. This contradiction is one of the main disagreements between *Ridley et al.* [1999] and *Lockwood and Cowley* [1999]. The data are explained by considering two processes, the rapid magnetosonic wave propagation of the enhanced cusp electric field and the slower redistribution of newly created open flux in the expanding polar cap.

[43] The magnetosonic wave appears to establish an afternoon convection cell almost immediately, but the flow appears to be parallel to the polar cap boundary at all local times in the field of view of the observations except near noon and in the closure of the cell on the nightside (>1900 MLT). We deduce that the movement

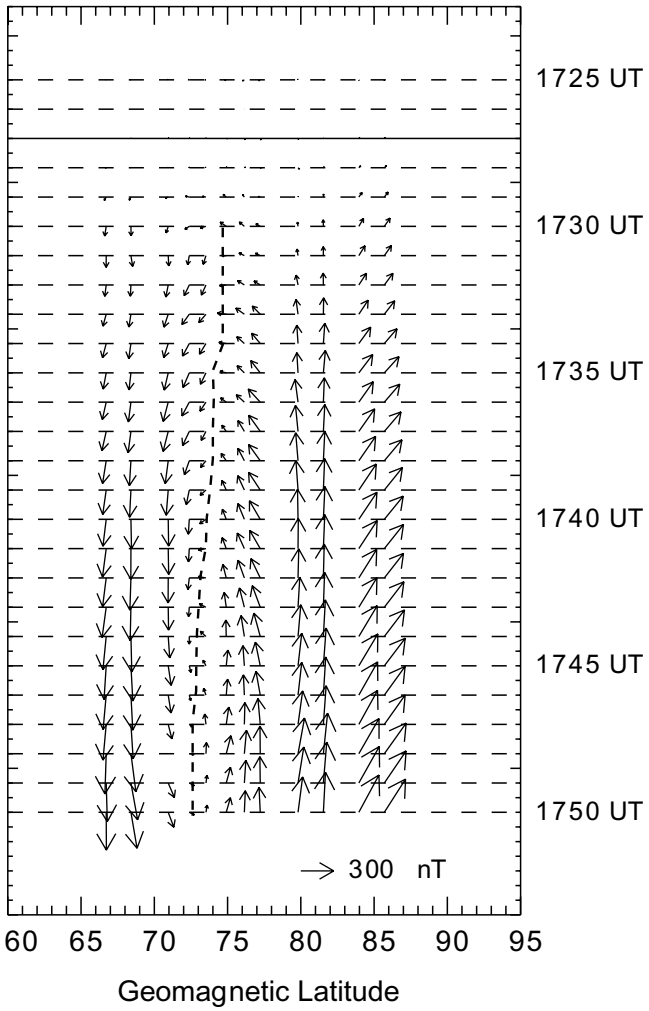

Figure 9. High-resolution (1-min) stack plot of Greenland West chain equivalent current vectors, located at ~1530 MLT. The westward component is upward, and the southward component is to the left. The baselines are set to the values at 1726 UT. The thick dashed line shows the estimated positions of convection reversal boundaries. The boundary is not drawn before 1730 UT because the changes were too small.

of the boundary in the 2100-MLT sector is due to an immediate enhancement of the plasma convection flow normal to the polar cap boundary (to 400 m/s). We assume that it is an adiaroic boundary (no flow across it). We do not have actual convection measurements here, but basically, the convective flow and the equatorward velocity of the boundary should be moving at the same speed. Thus no nightside reconnection needs to have started.

[44] The lack of an outstanding immediate response of the polar cap boundary in the 1500- to 1800-MLT sector must be because a much smaller plasma convection flow normal to the boundary is acting. This is different from, for example, Figure 3 of *Lockwood and Cowley* [1999], in which the flow normal to the boundary is initiated either side of noon and spreads toward the nightside.

[45] The critical point in the above is that the polar cap boundary moves rapidly only at noon and the nightside end of the afternoon convection cell. It would be difficult to consider this signature happening if the polar cap boundary were circular. For a short interval (until the CL1992 redistribution of newly created flux occurs, ~15 min) the polar cap in the afternoon cell must have been somewhat distorted, with the 1500-MLT sector at higher latitude than either the 1200-MLT or 2100-MLT sectors (Figure 10).

[46] In the present observation we find a rapid response along the axis of the noon/premidnight antisunward flow (~1100/~2100 MLT axis) and a much slower response in the dusk sector. The timescale of the response in the 1500- to 1800-MLT sector agrees with what is expected from the CL1992 model; that is, it is redistribution of the newly created open flux around the polar cap boundary.

[47] We should note that in discussing the boundary motion in the afternoon sector, we use the convection reversal and current reversal boundaries as proxies for the polar cap boundary, not the real ones. However, the separatrix positions inferred from the DMSP F13 particle data and the Stokkseyri convection reversal boundary show fairly good coincidence within 1° latitude, if we assume that the separatrix can be determined as the equatorward boundary of the SEZ region defined by a discontinuous decrease in $\gtrsim$1-keV plasma sheet electrons [*Lyons et al.*, 1996].

[48] The small IMF B_y for the first 5–7 min of the B_z southward period may account for some of the characteristics of this event. If there had been a large IMF B_y (causing flow oriented toward evening sector), then the polar cap boundary might have responded sooner. The zero IMF B_y (and later positive IMF B_y) means that flow is not directed toward the evening sector, i.e., there is very little flow component normal to the boundary, and hence little movement of the boundary is observed until redistribution of the new flux occurs.

[49] Note that DMSP F13 shows the Northern Hemisphere auroral oval/polar cap shifted toward dawn, as expected for IMF B_y positive [*Holzworth and Meng*, 1984]. The Southern Hemisphere should be shifted in the opposite sense, toward dusk, so Halley and Syowa should see a lower convection reversal boundary than Stokkseyri. However, both hemispheres show the equatorwardmovement of the polar cap boundary, so that the observation cannot be explained solely in terms of the B_y change effect. Most of the characteristics can be understood as resulting from the IMF B_z change only.

[50] *Ridley et al.* [1998] and *Ruohoniemi and Greenwald* [1998] did not observe the two-step response associated with the southward turning of the IMF that we see in the present study. One reason might be that the present event has a much larger IMF B_z change than the above studies. The B_z changes in their studies are 4 nT (+2 to −2 nT) and 10 nT (+5 nT to −5 nT), respectively, much smaller than the present change of 25 nT (+6 nT to −19 nT). This might lead to the difference in the observed characteristics of the ionospheric response.

[51] Figure 12 shows a schematic view of the interpretation of this event. The thick solid curve in the upper central panel shows the adiaroic boundary with no flow across it. The thick dashed line shows the merging gap with the flow across the boundary. The two-step response is interpreted in terms of the two different types of traveling disturbances. We speculate that the first response is associated with the propagation of fast magnetosonic waves in the magnetosphere. The second response is consistent with the CL1992 picture of the redistribution of the newly created open flux in the polar cap region.

4.2. Comparison With Previous Studies

[52] *Huang et al.* [1998] made a statistical study of the formation and decay of the quasi-stationary convection vortices (QSCVs) in the afternoon high-latitude ionosphere, after earlier observations reported by *Bristow et al.* [1995] and *Greenwald et al.* [1996]. Our example shows the large-scale convection pattern change in the noon to afternoon sector following a sudden southward turning of the IMF, so that there is a possibility that the convection pattern might include the effect of QSCV. However, since the most notable characteristic of our event

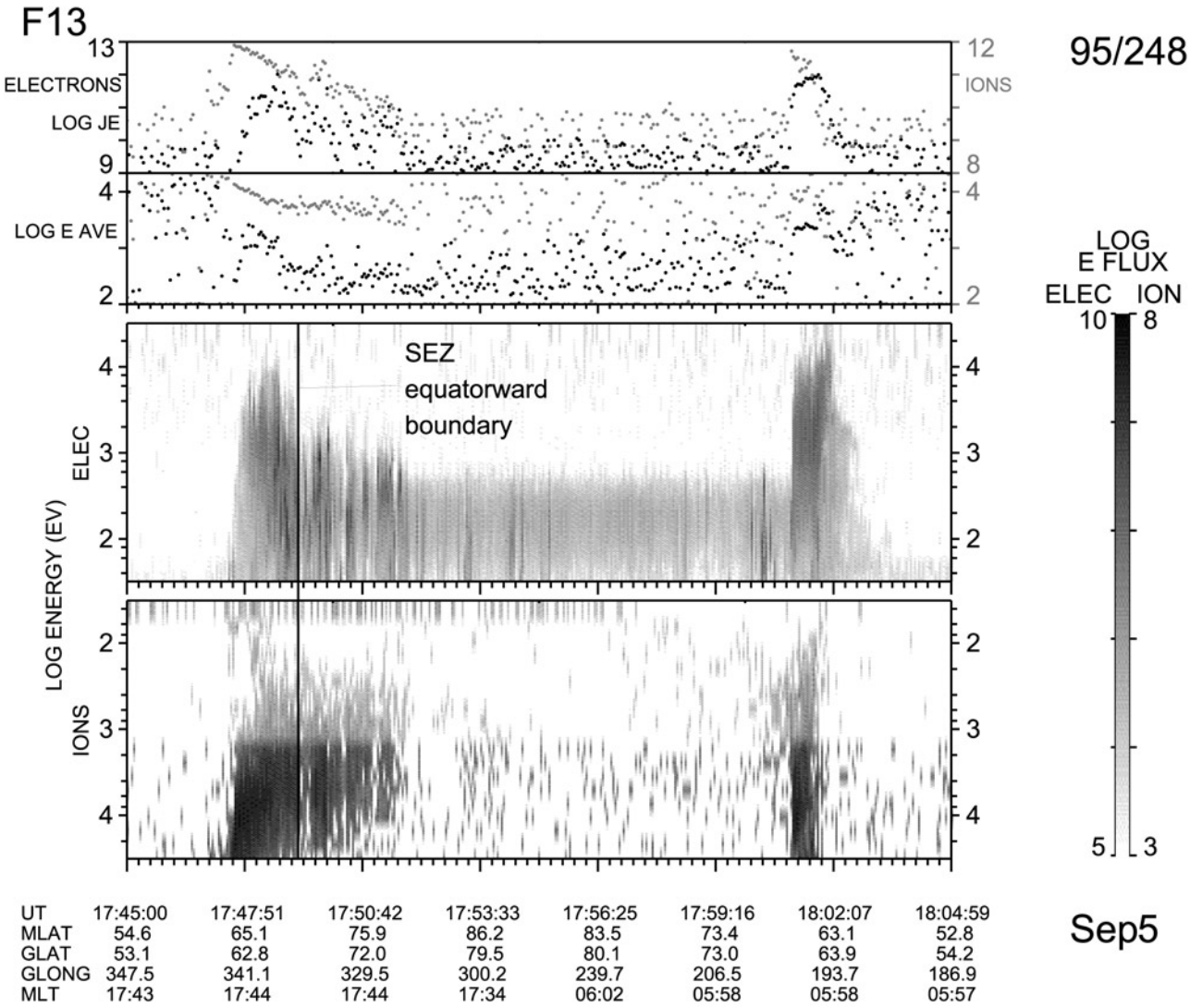

Figure 10. DMSP F13 ion and electron spectrograms during 1745–1805 UT. The vertical line indicates the estimated duskside equatorward boundary of the soft electron zone (SEZ), which is supposed to correspond to the separatrix.

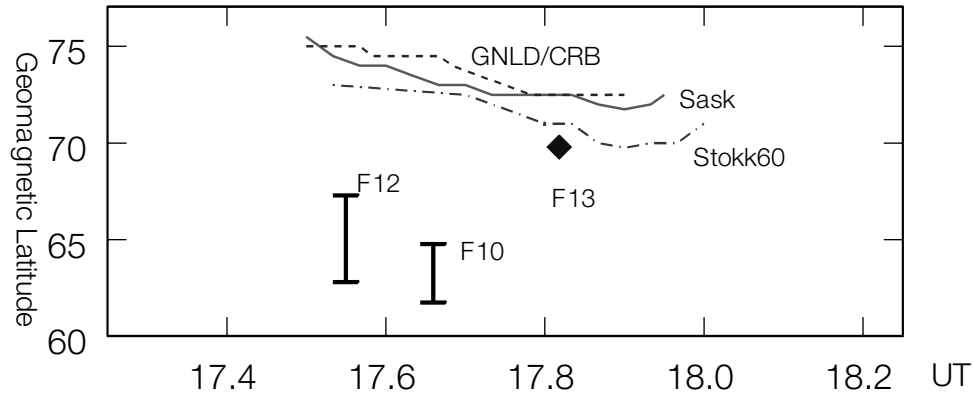

Figure 11. Stacked plot of Saskatoon cusp scatter boundary (solid line), Greenland West chain convection reversal boundary (dashed line), and Stokkseyri radar points at 60° longitude (dashed-dotted line). The vertical bars with ticks show DMSP F10/F12 auroral oval regions at ~2100 MLT in the Northern Hemisphere. The diamond shows the DMSP F13 separatrix in the dusk sector, as identified by the SEZ equatorward boundary. F12 is at 2036 MLT, F10 is at 2116 MLT, and F13 is at 1744 MLT.

Table 2. Summary of the Responses Associated With a Sudden Southward Turning of the IMF

	First Response (1728–1740 UT)	Delayed Response (1735–1750 UT)
Magnetic observation	formation of Dp-2 current vortices	equatorward expansion of the convection reversal boundary (1530 MLT)
Radar observation	formation of a flow vortex and equatorward shift of the cusp scatter region	equatorward expansion of the flow reversal boundary (~1700 MLT)
DMSP particle observation	equatorward expansion of nightside auroral oval	

during the delayed response is an equatorward afternoon convection cell expansion that progresses antisunward with time, it is unlikely that our event can be interpreted solely in terms of the appearance or the disappearance of a QSCV.

[53] *Ogino and Walker* [1998] proposed the idea of the convection front propagation on the basis of the MHD simulation results. They showed that the response time of the convection to the IMF southward turning is ~20 min. Their result agrees with that of *Walker et al.* [1999], who simulated the magnetospheric response to the rotating IMF in the *y-z* plane. The response time at the magnetopause in the $X = -20$ R_E region is between 15 and 30 min, which is consistent with the IMF travel time from the upstream boundary of the simulation box to $X = -20$ R_E. On the other hand, *Walker et al.* [1999] also showed that the response time of the plasma sheet configuration is ~1 hour. The main question is which part of the magnetosphere corresponds to the delayed response of the ionosphere in the dusk sector. The relationship of temporal sequence seems to indicate that the delayed response in the present study is more closely related to phenomena near the magnetopause region than to phenomena near the central plasma sheet region. This is reasonable because the most notable change in the delayed response in the ionosphere is the motion of the polar cap boundary (or its proxy).

5. Conclusions

[54] In response to a stepwise change in IMF B_z of +6 nT to −19 nT, we observed two stages of change in the ionospheric convection and the polar cap boundary in the afternoon sector. The initial formation of the vortex is immediate over a global scale, which is consistent with the earlier findings. The polar cap boundary in the noon and premidnight sectors also shows equatorward expansion almost simultaneously with the convection response.

[55] On the other hand, the polar cap boundary in the afternoon sector responds with a time delay of 10-20 min. This agrees with the results by *Etemadi et al.* [1988], *Todd et al.* [1988], and *Khan and Cowley* [1999]. This second response occurred ~10 min before the substorm expansion onset and does not seem to be related to a mechanism associated with substorm expansion onset. We conclude that the first response is consistent with the propagation of a magnetosonic wave and that the second response is consistent with the CL1992 theory of the redistribution of the newly created open flux in the polar cap region.

[56] Since it is difficult to find good examples of the large IMF stepwise change seen in the present case, only one event has been studied when the IMF suddenly turned southward. Nevertheless, this event provides a clue to the understanding of magnetospheric and ionospheric responses associated with a change in the external parameter.

[57] **Acknowledgments.** We thank all the staff who contributed to the operation of the SuperDARN radars. The Saskatoon radar operation is funded by grants from NSERC Canada. IMP 8 magnetic field data were provided by R. P. Lepping through the NSSDC, NASA/GSFC, and IMP 8 plasma data were obtained from MIT Space Plasma Physics Group. Wind magnetic field data were provided by R. P. Lepping through the NSSDC NASA/GSFC. Geotail magnetic field data were provided by S. Kokubun through DARTS at the Institute of Space and Astronautical Science (ISAS) in Japan. The MACCS magnetic data were provided by M. Engebretson at Augsburg College. The MACCS array is supported by U.S. National Science Foundation grants ATM-9610072 to Augsburg College and ATM-9704766 to Boston University. The Greenland magnetic data and the MAGIC array data were provided by DMI and University of Michigan, SPRL, respectively. The other magnetic field data used in this paper were obtained from the following organizations/people: INTERMAGNET;

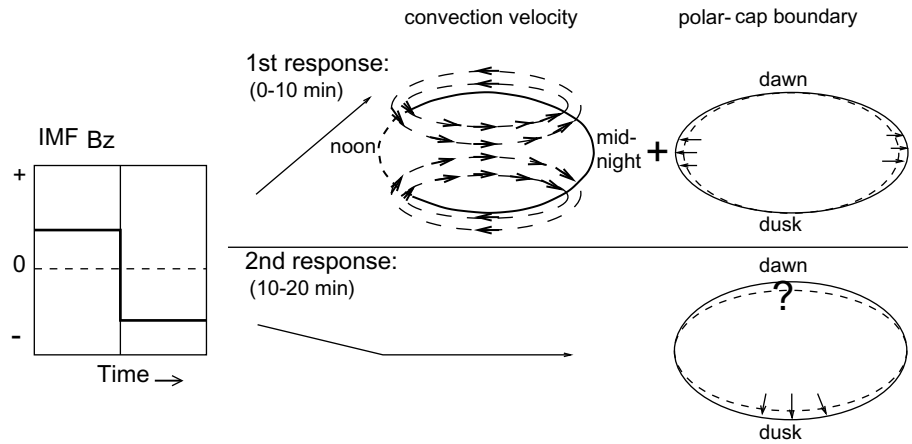

Figure 12. Schematic picture of the ionospheric response to an IMF southward turning. The thick solid curve in the upper central panel shows the adiaroic boundary with no flow across it. The thick dashed line shows the merging gap with the flow across the boundary.

WDC-C2 for Geomagnetism, Kyoto University; WDC-A, NGDC/NOAA. The DMSP particle data were provided by P. T. Newell at Applied Physics Laboratory, Johns Hopkins University.

[58] Hiroshi Matsumoto thanks A. Nishida and another referee for their assistance in evaluating this paper.

References

Araki, T., A physical model of geomagnetic sudden commencement, in *Solar Wind Sources of Magnetospheric Ultra-Low-Frequency Waves*, *Geophys. Monogr. Ser.*, vol. 81, edited by M. J. Engebretson, K. Takahashi, and M. Scholer, pp. 183–200, AGU, Washington, D. C., 1994.

Baker, K. B., and S. Wing, A new magnetic coordinate system for conjugate studies at high latitudes, *J. Geophys. Res.*, *94*, 9139–9144, 1989.

Baker, K. B., J. R. Dudeney, R. A. Greenwald, M. Pinnock, P. T. Newell, A. S. Rodger, N. Mattin, and C.-I. Meng, HF radar signatures of the cusp and low-latitude boundary layer, *J. Geophys. Res.*, *100*, 7671–7695, 1995.

Bristow, W. A., et al., Observations of convection vortices in the afternoon sector using the SuperDARN HF radars, *J. Geophys. Res.*, *100*, 19,743–19,756, 1995.

Cowley, S. W. H., and M. Lockwood, Excitation and decay of solar wind-driven flows in the magnetosphere-ionosphere system, *Ann. Geophys.*, *10*, 103–115, 1992.

Etemadi, A., S. W. H. Cowley, M. Lockwood, B. J. I. Bromage, D. M. Willis, and H. Lühr, The dependence of high-latitude dayside ionospheric flows on the north-south component of the IMF: A high time resolution correlation analysis using EISCAT "Polar" and AMPTE UKS and IRM data, *Planet. Space Sci.*, *36*, 471–498, 1988.

Greenwald, R. A., J. M. Ruohoniemi, W. A. Bristow, G. J. Sofko, J.-P. Villain, A. Huuskonen, S. Kokubun, and L. A. Frank, Mesoscale dayside convection vortices and their relation to substorm phase, *J. Geophys. Res.*, *101*, 21,697–21,713, 1996.

Hairston, M. A., and R. A. Heelis, Response time of the polar ionospheric convection pattern to changes in the north-south direction of the IMF, *Geophys. Res. Lett.*, *22*, 631–634, 1995.

Holzworth, R. H., and C.-I. Meng, Mathematical representation of the auroral oval, *Geophys. Res. Lett.*, *2*, 377–380, 1975.

Holzworth, R. H., and C.-I. Meng, Auroral boundary variations and the interplanetary magnetic field, *Planet. Space Sci.*, *32*, 25–29, 1984.

Huang, C.-S., G. J. Sofko, K. A. McWilliams, W. A. Bristow, R. A. Greenwald, and M. C. Kelley, SuperDARN observations of quasi-stationary mesoscale convection vortices in the dayside high-latitude ionosphere, *J. Geophys. Res.*, *103*, 29,239–29,252, 1998.

Kamide, Y., S.-I. Akasofu, and A. Brekke, Ionospheric currents obtained from the Chatanika radar and ground magnetic perturbations at the auroral latitude, *Planet. Space Sci.*, *24*, 193–201, 1976.

Khan, H., and S. W. H. Cowley, Observations of the response time of high-latitude ionospheric convection to variations in the interplanetary magnetic field using EISCAT and IMP-8 data, *Ann. Geophys.*, *17*, 1306–1355, 1999.

Lockwood, M., and S. W. H. Cowley, Comment on "A statistical study of the ionospheric convection response to changing interplanetary magnetic field conditions using the assimilative mapping of ionospheric electrodynamics technique" by A. J. Ridley et al., *J. Geophys. Res.*, *104*, 4387–4391, 1999.

Lockwood, M., A. P. van Eyeken, B. J. I. Bromage, D. M. Willis, and S. W. H. Cowley, Eastward propagation of a plasma convection enhancement following a southward turning of the interplanetary magnetic field, *Geophys. Res. Lett.*, *13*, 72–75, 1986.

Lopez, R. E., M. Wiltberger, J. G. Lyon, C. C. Goodrich, and K. Papadopoulos, MHD simulations of the response of high-latitude potential patterns and polar cap boundaries to sudden southward turnings of the interplanetary magnetic field, *Geophys. Res. Lett.*, *26*, 967–970, 1999.

Lyons, L. R., G. Lu, O. de la Beaujardière, and F. J. Rich, Synoptic maps of polar caps for stable interplanetary magnetic field intervals during January 1992 geospace environment modeling campaign, *J. Geophys. Res.*, *101*, 27,283–27,298, 1996.

Milan, S. E., T. K. Yeoman, and M. Lester, The dayside auroral zone as a hard target for coherent HF radars, *Geophys. Res. Lett.*, *25*, 3717–3720, 1998.

Ogino, T., and R. J. Walker, Response of the magnetosphere to a southward turning of the IMF: Energy flow and near Earth tail dynamics, in *SUBSTORMS-4*, edited by S. Kokubun and Y. Kamide, Kluwer Acad., Norwell, Mass., 1998.

Ohtani, S., R. D. Elphinstone, O. A. Troshichev, M. Yamauchi, L. Blomberg, L. J. Zanetti, and T. A. Potemra, Response of the dayside auroral and electrodynamic processes to variations in the interplanetary magnetic field, *J. Geophys. Res.*, *102*, 22,247–22,260, 1997.

Ridley, A. J., G. Lu, C. R. Clauer, and V. O. Papitashvilli, A statistical study of the ionospheric convection response to changing interplanetary magnetic field conditions using the assimilative mapping of ionospheric electrodynamics technique, *J. Geophys. Res.*, *103*, 4023–4039, 1998.

Ridley, A. J., G. Lu, C. R. Clauer, and V. O. Papitashvilli, Reply, *J. Geophys. Res.*, *104*, 4393–4396, 1999.

Ruohoniemi, J. M., and R. A. Greenwald, Statistical patterns of high-latitude convection obtained from Goose Bay HF radar observations, *J. Geophys. Res.*, *101*, 21,743–21,763, 1996.

Ruohoniemi, J. M., and R. A. Greenwald, The response of high-latitude convection to a sudden southward IMF turning, *Geophys. Res. Lett.*, *25*, 2913–2916, 1998.

Sandholt, P. E., et al., Cusp/cleft auroral activity in relation to solar wind dynamic pressure, interplanetary magnetic field B_z and B_y, *J. Geophys. Res.*, *99*, 17,323–17,342, 1994.

Saunders, M. A., M. P. Freeman, D. J. Southwood, S. W. H. Cowley, M. Lockwood, J. C. Samson, C. J. Farrugia, and T. J. Hughes, Dayside ionospheric convection changes in response to long-period interplanetary magnetic field oscillations: Determination of the ionospheric phase velocity, *J. Geophys. Res.*, *97*, 19,373–19,380, 1992.

Senior, C., D. Fontaine, G. Caudal, D. Alcayde, and J. Fontanari, Convection electric fields and electrostatic potential over $61° < \lambda < 72°$ invariant latitude observed with the European incoherent scatter facility, 2, Statistical results, *Ann. Geophys.*, *8*, 257–272, 1990.

Todd, H., S. W. H. Cowley, M. Lockwood, D. M. Willis, and H. Lühr, Response time of the high-latitude dayside ionosphere to sudden changes in the north-south component of the IMF, *Planet. Space Sci.*, *36*, 1415–1428, 1988.

Walker, R. J., R. L. Richard, T. Ogino, and M. Ashour-Abdalla, The response of the magnetotail to changes in the IMF orientation: The magnetotail's long memory, *Phys. Chem. Earth C*, *24*(1–3), 221–227, 1999.

Weimer, D. R., Models of high-latitude electric potentials derived with a least error fit of spherical harmonic coefficients, *J. Geophys. Res.*, *100*, 19,595–19,607, 1995.

N. Nishitani and T. Ogawa, Solar-Terrestrial Environment Laboratory, Nagoya University, Honohara 3-13, Toyokawa 442-8507, Japan. (nisitani@stelab.nagoya-u.ac.jp)

M. Pinnock, British Antarctic Survey, High Cross, Madingley Road, Cambridge CB3 OET, England, UK.

N. Sato and H. Yamagishi, National Institute of Polar Research, Tokyo 173-8515, Japan.

G. Sofko, Department of Physics and Engineering Physics, University of Saskatchewan, 116 Science Place, Saskatoon, Saskatchewan, Canada S7N 5E2.

O. Troshichev, Arctic and Antarctic Research Institute, 38 Bering Street, St. Petersburg 199397, Russia.

J.-P. Villain, Laboratoire de Physique et Chimie de l'Environnement, CNRS, 3A Avenue de la Recherche Scientifique, 45071 Orléans Cedex 2, France.

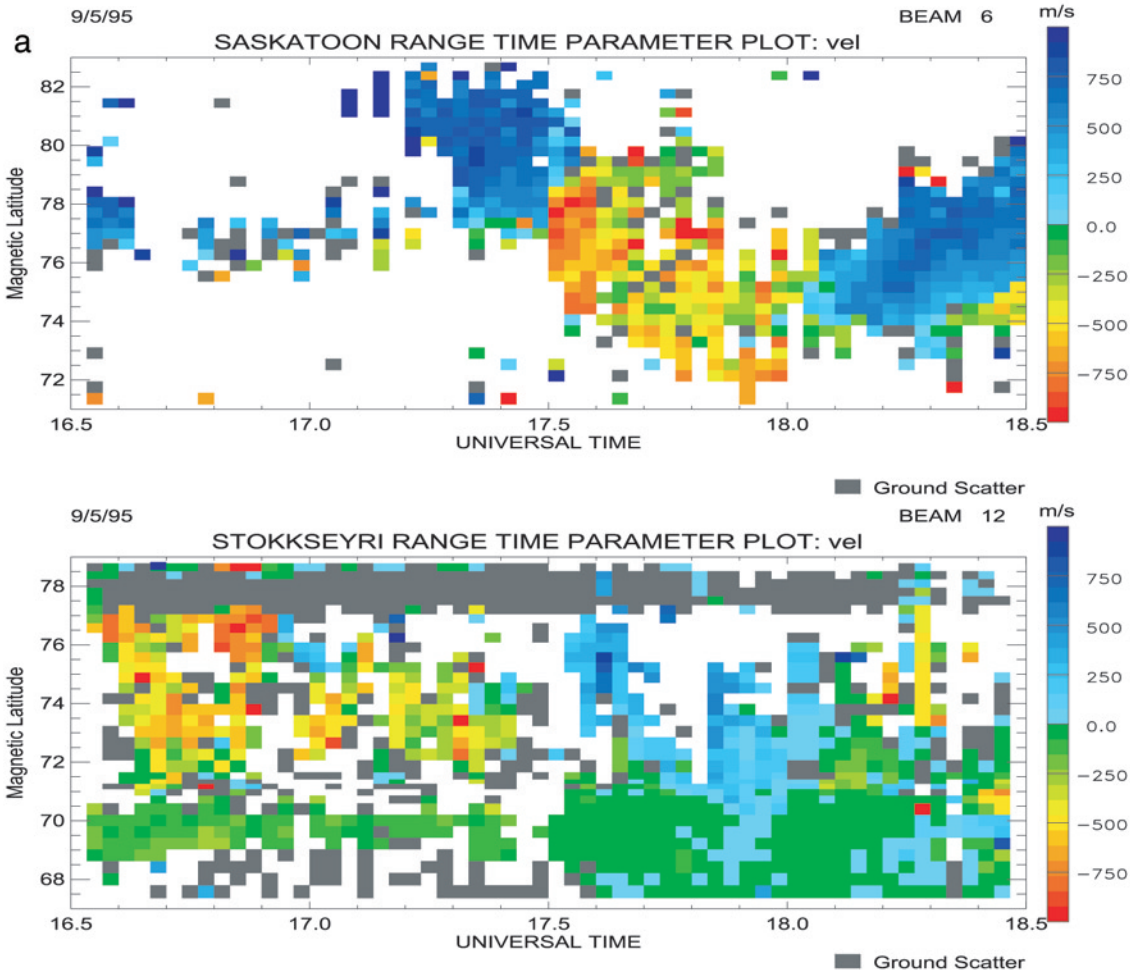

Figure 4. Range-time profile (RTP) plots of the line-of-sight velocities observed at beam 6 of the Saskatoon, beam 12 of the Stokkseyri, beam 8 of the Halley, and beam 13 of the Syoma radars from 1630 to 1830 UT. The positive velocities are toward the radar, and negative velocities are away from the radar. The gray area indicates a ground scatter region.

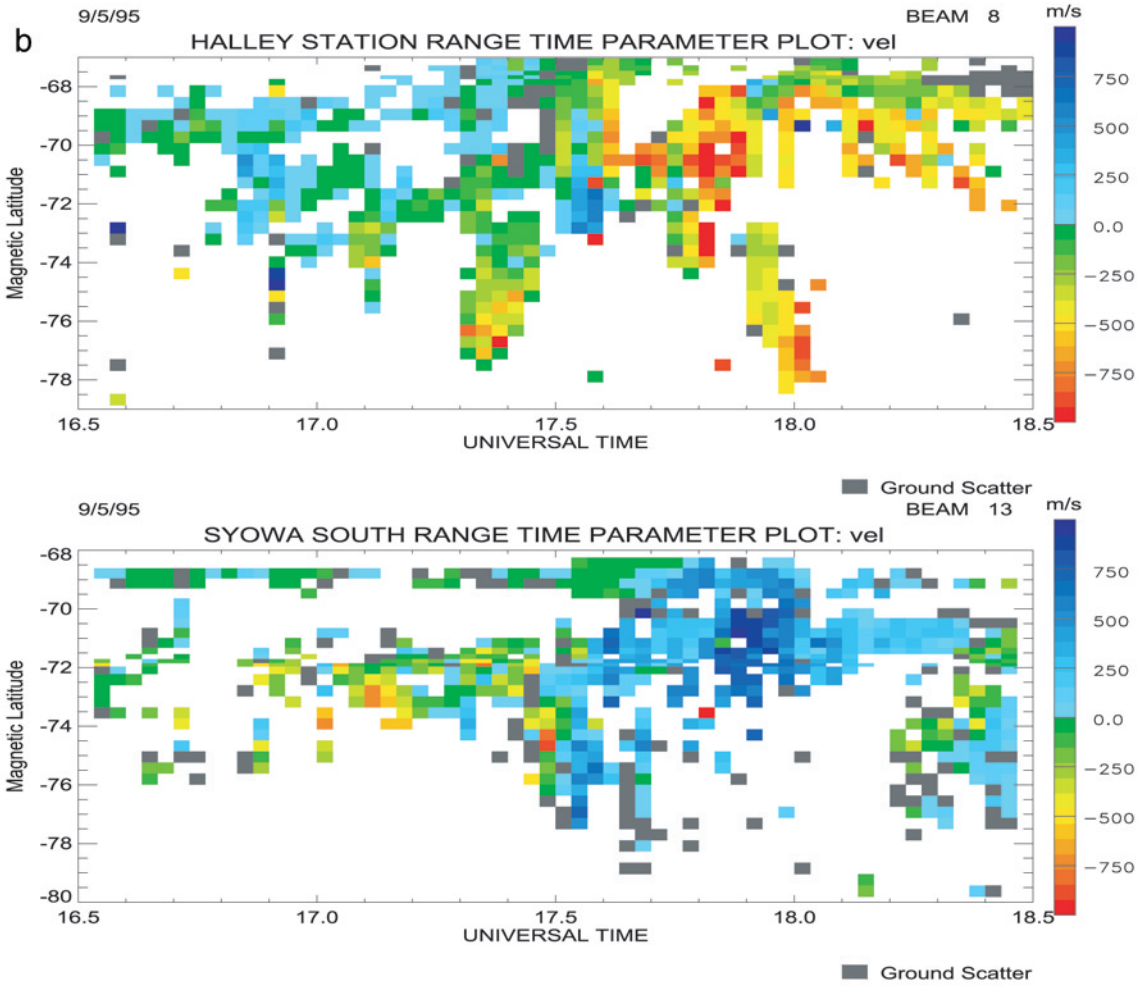

Figure 4. (continued)